Pressing Force Regulation in Robotic 3D Printing via CFD-Aided Nozzle Posture Control

Shinichi Ishikawa¹, Ryo Yamada¹, Wakana Tsuru² and Ryosuke Tasaki¹ Pepartment of Mechanical Engineering, Aoyama Gakuin University, Kanagawa, Japan Institute of Ocean Energy, Saga University, Saga, Japan

Keywords: Robotic 3D Printing, CFD Analysis, Force-Feedback Control, Extrusion Control, Force Sensing.

Abstract:

In the 3D printing process of applying materials, inadequate extrusion pressure critically deteriorates the deposition quality in robotic 3D printing. Feedback-based motion control with sensing and AI technology has been studied to respond to uneven and flexible surfaces, but challenges remain in optimizing the application force according to the situation. In this study, we investigate numerically and experimentally how the nozzle can change its orientation during the printing motion in a way that reduces the extrusion force. Numerical calculations are performed to derive the relationship between the clearance between the nozzle and the base and the extrusion force for multiple nozzle orientation patterns. Based on the numerical results, the relationship between the operating quantity (clearance) and the control quantity (maximum pressure and line width) is expressed mathematically to predict the quality model based on numerical fluid dynamics. In a variable-thickness printing experiment using a robot arm, a convex shape was reproduced by robot motion control that continuously changed the nozzle orientation. The experimental results demonstrated that adjusting the nozzle orientation effectively maintained extrusion force, preventing a reduction of approximately 0.01 N, as verified through force sensor-based inspection.

1 INTRODUCTION

3D printing technology is a processing method that creates 3D shapes by applying layers of material ejected from a nozzle (Volodymyr K. et al., 2024). Compared to conventional processing methods, this method allows for more flexible processing, making it suitable not only for desktop-scale printing but also for large-scale printing such as architectural 3D printing using concrete materials. Furthermore, as an advanced application of 3D printing technology, the technology is being developed for printing on the ground (Salvatore B. et al., 2024), curved surfaces (Jin Y. et al., 2016), and flexible surfaces (M. Miyatake et al., 2020). However, the effects of printing motion parameters and nozzle orientation on the shape of the printing line and the underlying foundation have not been fully elucidated.

Conventional additive technologies are mainly used for printing on a flat surface and in environments with little disturbance, and there are few examples of

printing on products or in environments with complex conditions. Feedback-based 3D printing methods using sensing methods (thickness control of printing lines (Rob J. et al., 2017), width control of printing lines (E. Shojaei et al., 2020), path change (S. Ishikawa et al., 2023), and feed rate change (Philip F. et al., 2022)) are being actively promoted to deal with printing methods in complex environments with a lot of uncertainty.

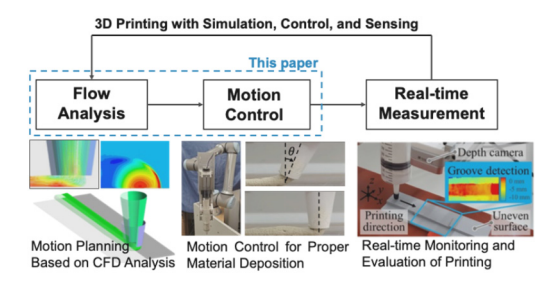


Figure 1: 3D printing process with CFD analysis and motion control.

alp https://orcid.org/0000-0002-8590-3019blp https://orcid.org/0000-0002-3619-4498

This study aims to clarify the effects of clearance and nozzle orientation on the extrusion force using numerical simulation and experiments. By conducting numerical simulation under multiple patterns of orientation angle conditions, the relationship between the amount of manipulation, including orientation and control in 3D printing is evaluated to achieve quality model prediction based on numerical fluid dynamics. The proposed 3D printing approach with CFD analysis and motion control is illustrated in Figure 1. In addition, a convex shape is produced by a printing experiment utilizing the orientation change of the nozzle by robot motion control, and the effect of the orientation change of the nozzle on the extrusion force is observed.

2 PRESSING FORCE CONTROL AND ROBOTIC-ARM-BASED 3D PRINTING SYSTEM

2.1 Robotic-Arm-Based 3D Printing and Force Measurement System

The Robotic-arm-based 3D printing system and the measurement device for extrusion force measurement are shown in Figure 2. The extruder using a stepping motor is installed at the end of a 6-DOF robot arm to perform multi-axis dispensing motions. A force sensor with a fixed acrylic plate is used to measure the force with which the dispensed material is applied.

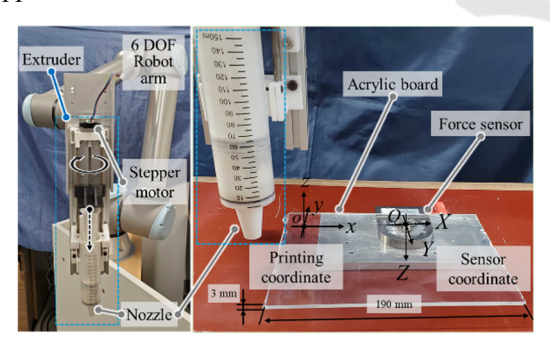


Figure 2: Appearance of the dispensing mechanism with force measurement device.

A 6-axis force sensor with a rated capacity of ± 50 N in the Z-direction and a resolution of 1/4000 was employed. Sensor values are measured in a PC with a low-pass filter to remove noise.

Mortar putty (HI Level Super, KLASS) is used as a printing material, which possesses specific viscosity and yield value, making it suitable for construction

applications. The powdered putty is combined with water, loaded into a syringe, and then dispensed. Upon contact with water, the material undergoes a reaction and solidifies after a certain period.

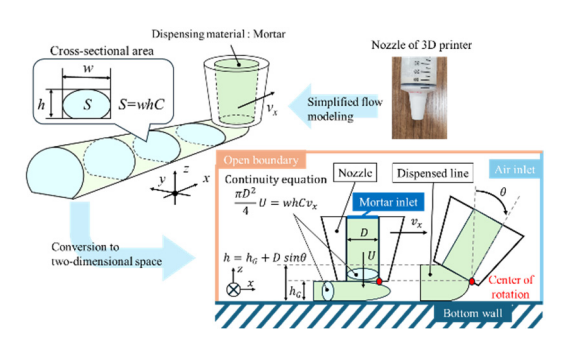


Figure 3: Simplified flow rate model for determining dispensing operations.

2.2 Simplified Flow Rate Model for Determining Dispensing Operations

A simplified flow rate model was developed to determine the dispensing operation based on nozzle movement, including nozzle orientation. The relationship between the shape of the dispensed line formed by dispensing, and printing parameters such as clearance and nozzle orientation angle, is represented as shown in Figure 3. Since the discharge flow rate from the nozzle is equal to the dispensed flow rate, this relationship can be expressed by the continuity equation as shown in Equation (1).

In the simplified flow rate model represented by Equation (1), the discharge flow velocity of the material is denoted as U [mm/s], the nozzle diameter as D [mm], and the nozzle feed velocity as v_x [mm/s]. The dispensed line width, thickness, and cross-sectional area correction coefficient are denoted as W [mm], h [mm], and C [-], respectively. Based on our previous research(S. Ishikawa et al., 2025), the value of C is assumed to be 0.8.

In the proposed convex shape printing method, convex shapes are formed by altering the thickness through changes in nozzle orientation. To establish a one-to-one relationship between the rotation direction and clearance variation, the rotation center during nozzle orientation changes is set at the edge of the nozzle outlet, as illustrated in Figure 3.

$$(\pi D^2 U)/4 = hwCv_x \tag{1}$$

$$h = h_G + D\sin\theta \tag{2}$$

The line thickness h of the printed structure is determined by the sum of the clearance h_G at the lowest point of the nozzle outlet and the clearance

variation due to the orientation angle θ . The dispensing operation is determined using this relationship. The correlation between clearance and line thickness is expressed in Equation (2).

3 NUMERICAL SIMULATION OF DISPERSED MATERIAL

Using numerical simulation software, the effect of the proposed convex-shape printing operation on mortar putty was analysed. Pressure distribution changes during clearance increases and nozzle orientation changes are visualized.

3.1 Numerical Calculation Method

Numerical calculations were conducted to visualize pressure distribution. As shown in Figure 3, the mortar putty is discharged from the nozzle outlet and flows outside the calculation domain. The calculation focused on a steady-state flow within the domain. The calculation domain is indicated in Figure 4. The steady, incompressible Navier-Stokes equations for mortar putty-air two-phase flow were solved using Ansys Fluent 2024 R2. The calculation conditions are summarized in Table 1.

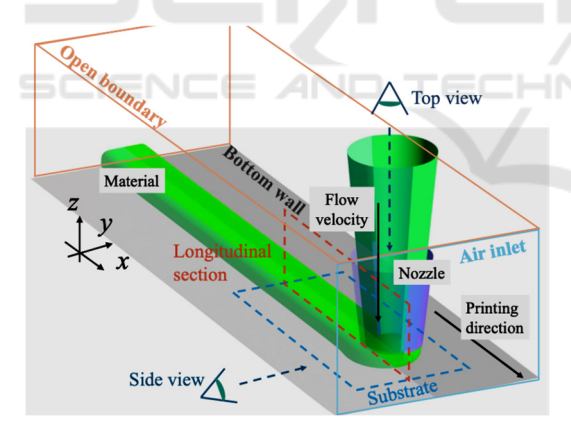


Figure 4: Calculation domain for simulate of 3D printing process.

Table 1: Main parameters of 3D printing simulation.

Nozzle diameter D [mm]	10
Feed velocity v_x [mm/s]	10
Dispensing velocity U [mm/s]	5.3
Clearance h_G [mm]	4
Nozzle orientation angle θ [$^{\circ}$]	0
Density ρ [kg/m ³]	800
Viscosity μ [kg/(m · s)]	1000
Gravitational acceleration g [m/s ²]	9.81

The viscosity of the mortar putty was estimated based on literature values (N. Izumo et al., 2008), and its density was measured from the bulk density. Since the flow of mortar putty is dominated by viscous forces over inertial forces, it was treated as laminar. For this flow analysis, the Volume of Fluid (VoF) model, a type of two-phase flow calculation model, was utilized. Assuming symmetry in the *z-x* plane, only half of the domain was solved. A structured grid with 250,000 nodes was employed.

The z-x plane was set as a symmetry boundary, and the average velocity of mortar putty at the nozzle outlet tip, as shown in Table 1, was applied at the inlet boundary in Figure 4. The lower wall velocity was set to $-v_x$, solving the flow in the relative coordinate system of the nozzle. For the air flow outside the nozzle, the right boundary of Figure 3 was set as an inlet boundary for air with a velocity of $-v_x$.

The nozzle and lower wall were treated as no-slip walls, while other surfaces, including the mortar-air boundary, were treated as open to the atmosphere. The computational domain reflecting these conditions is illustrated in Figure 4.

3.2 Pressure Distribution Changes by Nozzle Orientation

The effects of conventional 3-degree-of-freedom printing and the proposed multi-degree-of-freedom printing methods on discharged materials were investigated through numerical simulation. Based on the simplified flow rate model in Equation (1), a scenario was considered where the printed line

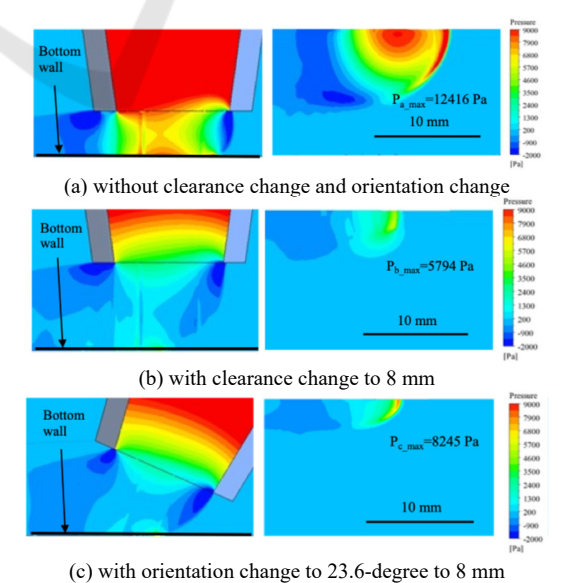


Figure 5: Pressure distribution in longitudinal section and

on substrate.

thickness varies from 4 mm to form a convex shape. Two cases were compared: increasing the clearance from 4 mm to 8 mm to achieve a 4 mm thickness increase and altering the nozzle orientation to achieve the same thickness increase.

For the conditions in Table 1, Figure 5(a) shows the pressure results obtained by the simulation for the vertical and bottom surfaces of half the domain. Figures 5(b) and (c) depict the results for an 8 mm clearance increase and a 23.6° nozzle orientation change, respectively. Comparing Figures 5(b) and (c), the positive pressure distribution range of the mortar putty in contact with the bottom surface was broader in the clearance increase case. However, the maximum pressure was 8,245 Pa in the nozzle orientation case and 5,794 Pa in the clearance increase case, showing a 1.42-fold higher pressure in the former.

4 MEASUREMENT OF PRESSING FORCE IN CONVEX SHAPE PRINTING

In convex printing using nozzle orientation changes, multiple convex shapes were reproduced to investigate the effect of nozzle orientation changes on extrusion force. The extrusion force was extracted from the load values.

4.1 Experimental Conditions

Using the experimental setup shown in Figure 2, the extrusion force during the printing of identical convex shapes was measured and compared for cases of clearance change alone and nozzle orientation change alone. Both the clearance and orientation change cycles were 4 seconds, with convex shapes formed at four locations. Other printing parameters were determined by referencing section 3 to match numerical calculation conditions.

4.2 Results of The Convex Shape Printing Experiment

The printed line appearances for each operation are shown in Figure 6, and the Z-direction load measurements from the force sensor are presented in Figure 7. Figure 7(a) confirms that extrusion force decreases during convex shape printing. Figure 7(b) extracts extrusion force changes by subtracting sensor values during printing without clearance or orientation changes. It shows that the reduction in

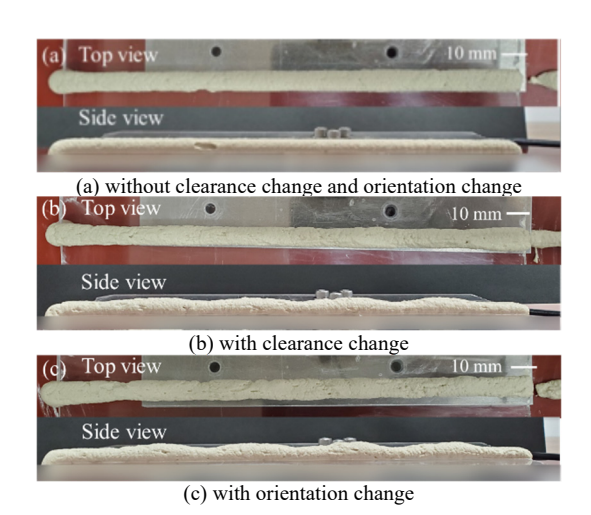
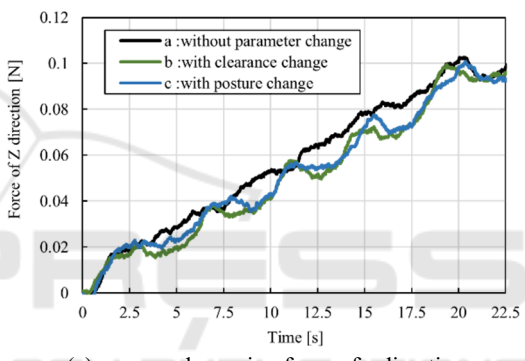
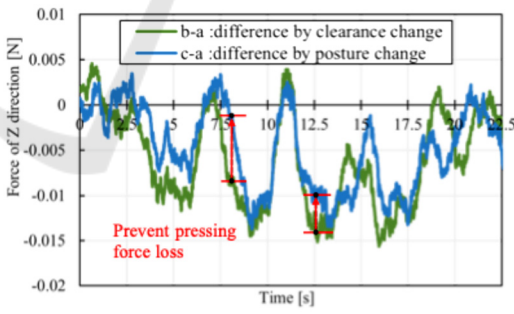


Figure 6: Printed line by printing motion with clearance and orientation change.



(a) measured pressing force of z direction



(b) difference in each force of z direction

Figure 7: Comparison of measured pressing forces by each printing motion.

extrusion force during convex shape printing is approximately 0.01 N smaller in the nozzle orientation case than in the clearance change case. This suggests that limiting clearance increases through orientation changes can mitigate extrusion force reduction.

Furthermore, this experimental tendency is consistent with the CFD analysis presented in Section

3. The numerical results indicated that, for the same convex height increase, the nozzle orientation change produced a more concentrated pressure distribution and a higher maximum pressure (1.42 times greater) compared to the clearance increase case. The experimental observation of smaller force reduction therefore supports the simulation outcome, confirming that nozzle orientation control effectively maintains extrusion pressure. This agreement between simulation and experiment demonstrates that the CFD-derived pressure distribution can serve as a predictive model for extrusion force behavior in robotic 3D printing.

5 CONCLUSIONS

In this study, a 3D printing method utilizing nozzle orientation changes via a robotic arm was verified through numerical simulation and physical experiments to suppress the decrease in extrusion force and achieve high-quality 3D-printed structures. In the numerical simulation, the effect of the clearance between the nozzle and the base on the extrusion force was evaluated, considering multiple nozzle orientation angles. Furthermore, it was confirmed that the maximum pressure becomes 1.42 times greater during orientation changes compared to clearance changes, indicating its contribution to the local enhancement of the extrusion force.

Furthermore, in experiments using robotic motion control, the printing of convex shapes was successfully reproduced through continuous nozzle orientation changes. Quality inspection utilizing a force sensor confirmed that the proposed printing method suppressed the reduction in extrusion force by approximately 0.01 N.

In this paper, a new 3D printing framework based on CFD analysis is introduced, and this study provides novel insights into the effect of nozzle orientation on extrusion force during robotic 3D printing. These findings highlight a novel design perspective in robotic 3D printing that leverages multi-axis motion planning informed by fluid dynamics.

REFERENCES

Jin Yuan, Jianke Du, Yong He, and Guoqiang Fu (2016). Modeling and process planning for curved layer fused deposition, *The International Journal of Advanced Manufacturing Technology*, Volume 91, pp. 273–285.

- Mako Miyatake and Aoi Watanabe (2020). Interactive cake decoration with whipped cream, *ICMR* '20: International Conf. on Multimedia Retrieval, pp. 7–11.
- Naoto Izumo and Hisanori Oda (2008). Observing the cure processes of cement materials based on static viscosity measurements, *Ceramics Japan*, Volume 3.
- Philip F. Yuan, Qiang Zhan, Hao Wu, Hooi Shan Beh, and Liming Zhang (2022). Real-time toolpath planning and extrusion control (RTPEC) method for variable-width 3D concrete printing, *Journal of Building Engineering*, Volume 46, 103716.
- Rob J. M. Wolfs, Freek P. Bos, Emiel C. F. van Strien, and Theo A. M. Salet (2017). A real-time height measurement and feedback system for 3D concrete printing, *High Tech Concrete: Where Technology and Engineering Meet*, pp. 2474–2483.
- Salvatore Bruno, Giuseppe Cantisani, Antonio D'Andrea, Kristian Knudsen, Giuseppe Loprencipe, Laura Moretti, et al. (2024). A small robot to repair asphalt road potholes, *Infrastructure*, Volume 9, pp. 210–227.
- Shinichi Ishikawa, Takahito Yamashita, and Ryosuke Tasaki (2023). Vision-based monitoring and control for 3D printing process with dynamic ROI and path modification algorithm, *Journal of Advances in Information Technology*, Volume 14, No. 6, pp. 1443–1449
- Shinichi Ishikawa, Ryo Yamada, and Ryosuke Tasaki (2025). High-sensitivity Interlayer Force Measurement and Multi-layer Smoothing Control for 3D Printing on Uneven Surfaces, SICE Journal of Control, Measurement, and System Integration, Volume 18, Issue 1.
- Shojaei Barjuei, E., Courteille, E., D. Rangeard, F. Marie, and A. Perrot (2020). Real-time vision-based control of industrial manipulators for layer-width setting in concrete 3D printing applications, *Advances in Industrial and Manufacturing Engineering*, Volume 5, 100094
- Volodymyr Khyzhynskyi, Mykola Lampeka and Valerii Strilets (2024). The history of the development of 3D printing technologies and their use in world artistic ceramics, *History of science and technology*, Volume 14, issue 1, pp. 152-183.